









# Hemocompatibility of Differently Modified Polymeric Nanofibers: Current Progress in the Biomedical Industry

# 10

Rumysa Saleem Khan , Anjum Hamid Rather ,  
Taha Umair Wani , Muheeb Rafiq , Touseef Amna ,  
M. Shamshi Hassan , Syed Mudasir Ahmad, Shafquat Majeed,  
Mushtaq A. Beigh, and Faheem A. Sheikh

## Abstract

Any implant intended for tissue engineering application should be blood compatible. Since nanofibers are used as suitable candidates for applications where they are directly exposed to blood, the fabrication of nanofibers with excellent blood compatibility has been an unmet challenge for all tissue engineering applications. In this regard, various nanofibers have been fabricated through electrospinning

R. S. Khan · A. H. Rather · T. U. Wani · M. Rafiq · F. A. Sheikh (✉)  
Department of Nanotechnology, University of Kashmir Hazratbal, Srinagar, Jammu and Kashmir, India  
e-mail: [rumysakhan.scholar@kashmiruniversity.net](mailto:rumysakhan.scholar@kashmiruniversity.net); [anjumhamid.scholar@kashmiruniversity.net](mailto:anjumhamid.scholar@kashmiruniversity.net); [wanitaha.scholar@kashmiruniversity.net](mailto:wanitaha.scholar@kashmiruniversity.net); [muheeb.ntjrf@uok.edu.in](mailto:muheeb.ntjrf@uok.edu.in); [faheemnt@uok.edu.in](mailto:faheemnt@uok.edu.in)

T. Amna  
Department of Biology, Faculty of Science, Albaha University, Albaha, Kingdom of Saudi Arabia

M. S. Hassan  
Department of Chemistry, Faculty of Science, Albaha University, Albaha, Kingdom of Saudi Arabia

S. M. Ahmad  
Faculty of Veterinary Sciences, Sher-e-Kashmir University of Agricultural Sciences and Technology, Srinagar, Jammu and Kashmir, India  
e-mail: [mudasirbio@skuastkashmir.ac.in](mailto:mudasirbio@skuastkashmir.ac.in)

S. Majeed  
Laboratory for Multifunctional Nanomaterials, Department of Nanotechnology, University of Kashmir Hazratbal, Srinagar, Jammu and Kashmir, India  
e-mail: [smshah@uok.edu.in](mailto:smshah@uok.edu.in)

M. A. Beigh  
Cellular Signalling and Nanotherapeutics Laboratory, Department of Nanotechnology, University of Kashmir Hazratbal, Srinagar, Jammu and Kashmir, India  
e-mail: [beighm@uok.edu.in](mailto:beighm@uok.edu.in)

while incorporating different factors for enhancing blood compatibility. Recent studies have demonstrated the use of various contrasting agents for modifying the properties of tissue scaffolds. In this chapter, natural and synthetic polymers that are fabricated into nanofibers are discussed for their role in blood compatibility. The choice of polymer used, that is, natural or synthetic; the use of drugs, such as aspirin; the growth factors incorporated in it, like vascular endothelial growth factor; and the topography of scaffolds, for example, smooth and rough, have a significant impact on blood compatibility. This chapter focuses on the characteristics of scaffolds, the methods of preparation, and the factors incorporated in these nanofibers that influence hemocompatibility. A detailed account of different assays employed in analyzing blood compatibility has also been discussed, such as the determination of the hemolysis rate, platelet adhesion, plasma recalcification time, free hemoglobin estimation, the attachment and release of red blood cells, and the adsorption of plasma proteins.

### Keywords

Blood · Hemocompatibility · Drug delivery · Nanofibers · Scaffolds · Clotting · Electrospinning · Polymers

## 10.1 Introduction

Nanofibrous scaffolds are highly porous with a large surface area and have excellent permeability. Henceforth, nanofibers are considered potential candidates for adsorption applications (Sahay et al. 2012). Electrospinning is one of the most robust methods of nanofiber fabrication compared to other techniques. It is easy, economical, and highly versatile in forming nanofibers using various polymers. These nanofibers can act as scaffolds, which are supposed to closely mimic the components of the extracellular matrix (ECM) (Pham et al. 2006; Sell et al. 2007). The setup for the process of electrospinning is shown in Fig. 10.1. Synthetic polymers, such as

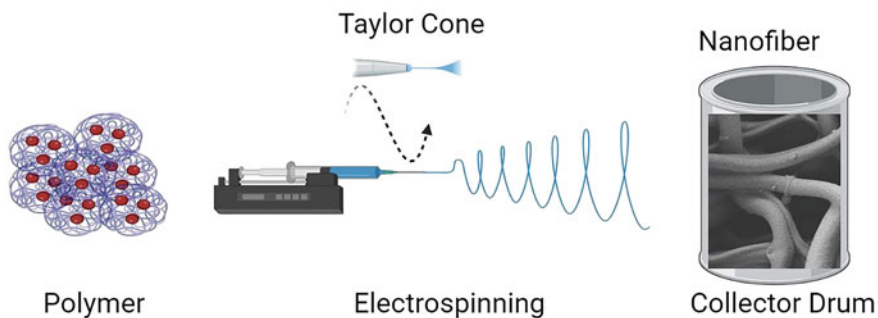


**Fig. 10.1** The pictorial presentation of polymer electrospinning. The polymers can be synthetic or natural, which should be completely soluble in solvents. This polymer solution can be filled in a syringe, which, under the influence of a high voltage, is ejected into nanofibers that are collected on the metal collector

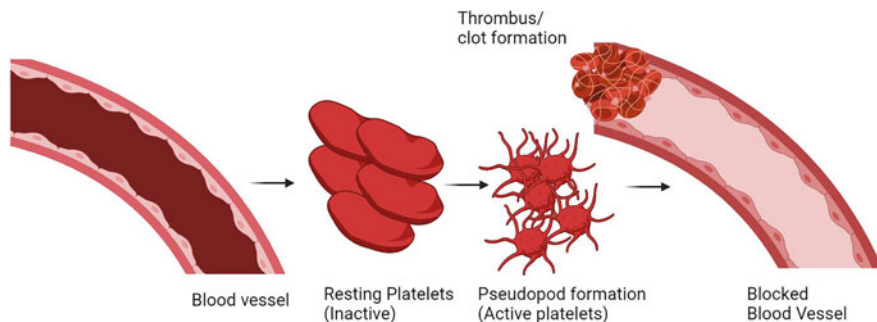


**Fig. 10.2** Schematic showing the processes of platelet activation and thrombus formation

polyurethane, which has excellent biocompatibility (Lluch et al. 2013); polyvinyl alcohol, which has high mechanical strength and elasticity (Xu et al. 2008); polyether sulfone, which has good mechanical properties and high thermal stability (Hou et al. 2008); poly(vinyl pyrrolidone), having the property of amphiphilicity, inertness, and chemical stability (Kurakula and Koteswara Rao 2020); and poly(lactic acid), being thermoplastic with high biocompatibility and biodegradability, are widely used in the preparation of nanofibers through electrospinning, are sought after in biomedical applications. On the other hand, natural polymers, such as chitosan (Dash et al. 2011), silk fibroin (Nguyen et al. 2019), cellulose (Seddiqi et al. 2021), etc., are also widely used in bioengineering applications due to their biocompatible and biodegradable character. Chitosan is the only primary polysaccharide with good biocompatibility and biodegradability; additionally, it possesses antifungal properties (Li et al. 1992).

As aforementioned, these synthetic or natural polymers can be fabricated into nanofibers using the electrospinning technique for various applications. However, the fabrication of nanofibers with robust blood compatibility remains an unmet goal in the biomedical field (Soundararajan et al. 2018). On the contact of blood with foreign material (which can be undesired nanofibers), a cascade of lethal effects can occur, for instance, adsorption of plasma proteins, platelet accumulation, and, finally, thrombus or clot formation (Fig. 10.2) (Gorbet and Sefton 2006). Contrary to this, it has been observed that the plasma proteins and platelets present in the blood are readily adsorbed on these polymeric nanofiber surfaces (Gorbet and Sefton 2006; Ren et al. 2013). For example, the positively charged chitosan readily adsorbed negatively charged proteins, which caused platelet activation and thrombus formation. However, at the same time, it preferably bound human serum albumin, reducing platelet attachment and activation (Lv et al. 2017; Balan and Verestiuc 2014). Various efforts have been put forward to modify the blood compatibility of polymeric nanofibers, such as polyurethane, through the introduction of surface additives (Hsiao et al. 2015; Chen et al. 2011). To improve compatibility with blood, the electrospun mats have been functionalized by adsorbing certain moieties, like those of antithrombogenic factors (Freitas et al. 2010), moieties of bioinert and inorganic materials, (Hauert 2005), and organic coatings (Kim and Kim 2002) or by preparing cell-friendly surfaces (Qi et al. 2013). Similarly, chitosan, its composites,

and derivatives modified with different functional groups are fabricated (Balan and Verestiuc 2014; Yang et al. 2007). The negative  $-\text{SO}_3^-$  or  $-\text{COO}^-$  groups in functionalized chitosan have good blood compatibility because of negative charges, which lower the attachment of plasma proteins that have negative charges on their surfaces (Sagnella and Mai-Ngam 2005). Silk fibroin is another natural polymer widely used in biomaterials fabrication due to its excellent biocompatibility and biodegradability (Naskar et al. 2017a, b). The hemolysis of blood is a significant parameter for checking compatibility with biomaterials. If the material has excellent hemocompatibility, there is no hemolytic phenomenon or platelet adsorption on the surface. Upon hemolysis, hemoglobin is released into the plasma following the damage of membranes of red blood cells, which is directly associated with the compatibility of material (Song et al. 2016). There are several methods for determining the blood compatibility of samples in a laboratory, including measuring the hemolysis rate. The hemolysis rate measures the extent of lysed red blood cells (RBCs) upon the contact of the sample with blood. The lesser the hemolytic rate is, the greater is the blood compatibility of samples. An ideal biomaterial should have a hemolysis rate of less than 5% (Song et al. 2016). Another method includes the proliferation of platelets on the nanofiber surface. The spreading of platelets and their aggregation are major confirmatory indications of platelet activation and are taken as the chief pathway of thrombosis. The attachment of blood platelets is a spontaneous approach to measuring the compatibility of materials (He et al. 2011). The thrombogenicity indicator of a material in a blood compatibility experiment is given by the number of platelets that attach on the surface and the altered shape of those platelets on coming in contact of the material with the blood. Upon contact of foreign material with blood, the first response is the adsorption of serum proteins and the subsequent platelet adhesion and activation of coagulation pathways, which finally result in thrombus formation (Huang et al. 2011). The Vroman effect is the consequence of the hydrophilicity and topography of material surfaces (De Mel et al. 2012). Moreover, the adsorption of plasma proteins is an indispensable parameter in evaluating the thrombogenicity of materials. The blood plasma consists of several proteins, such as albumin (45 mg/mL), immunoglobulin G (10 mg/mL), fibrinogen (3 mg/mL), transferrin (3 mg/mL), and immunoglobulin A (1 mg/mL) (Vogler 2012). Upon the contact of blood with the biomaterial, initially, the proteins adsorb onto the surface, which leads to the recruitment of platelet, white blood cells (WBCs), and red blood cells (RBCs). Finally, adhesion on the plasma protein layer occurs, leading to the formation of thrombin (Vogler 2012). The adsorption of protein in blood plasma increases with the hydrophilicity and causes unwanted thrombus formation events. Furthermore, the stress on the cells is dependent on the roughness of the substrate, which later increases hemolysis (Leszczak et al. 2013). Different strategies have been used to prevent protein and platelet attachment on the biomaterials to attain hemocompatibility and anticoagulation (Weber et al. 2002). Another method involves the assessment of the anticoagulant characteristics of the substrate by recording free hemoglobin in the blood (Soundararajan et al. 2018). In this method, coagulation is initiated, which leads to the formation of a stabilized fibrin clot formed by RBCs, WBCs, and platelets. Then the release of hemoglobin from the clot is measured, which determines the anticoagulant property.

Furthermore, how much the given biomaterial sample causes a delay in the clotting of platelet-poor plasma (PPP) is measured by plasma recalcification time (PRT), which causes the activation of prothrombin (factor II) on the addition of  $\text{Ca}^{2+}$ . PRT gives the point of delay in the coagulation process (Soundararajan et al. 2018). In this method, the time taken by the sample in showing the first signs of fibrin thread formation is observed. When the sample contacts with PPP, it can signal the intrinsic coagulation pathway, given that coagulation factors are present. Blood compatibility is also determined by the adsorption of blood proteins on biomaterials (Wei et al. 2009; Denis et al. 2002; Scopelliti et al. 2010). In this chapter, we discuss the impact of different electrospun nanofibers with different modifications on checking blood compatibility. This chapter will provide readers an insight into the different strategies for modifying nanofibers and their evaluation by different hemocompatibility assays for use in biological applications.

---

## 10.2 Effect of Drug-Loaded Nanofibers on Blood Compatibility

Poly(lactic acid) and silk fibroin nanofiber mats of different mass compositions loaded with aspirin for their anticoagulant property have been prepared by electrospinning (Qin et al. 2013). In designing the solutions for electrospinning, the solvent used was trifluoroacetic acid and dichloromethane in the proportion of 70 parts:30 parts. Poly(lactic acid) was used due to its potential for the controlled release of drugs in the form of fibroin scaffolds, electrospun mats, microspheres, and films (Dev et al. 2010; Kim et al. 2010; Nagarwal et al. 2011). However, due to its low biological activity and hydrophobicity, cell attachment is cumbersome. Therefore, they incorporated poly(lactic acid) in fibrous protein (i.e., silk fibroin), which is hydrophilic, inducing low to no immunogenic response. In addition, it exhibits flexible degradation rates, fluctuating from days to months in vivo due to enhanced crystallinity (Fei et al. 2011). However, regenerated silk fibroin has low mechanical properties because of the modifications in conformations and the distortion of molecules (Li et al. 2011). This led the researchers to blend poly(lactic acid) and silk fibroin into a composite nanofiber mat for the fabrication of biomaterial with the required properties. After degumming and dialysis, the silk fibroin solution was filtered and freeze-dried to get silk fibroin sponges. Then different solutions containing different compositions of poly(lactic acid)/silk fibroin (8/1, 8/3, and 8/5) and aspirin (0.7%, 0.9%, and 1.1%) were prepared. It was observed that when silk fibroin concentration was increased, the degree of compatibility in poly(lactic acid) and silk fibroin was reduced and resulted in increased diameters in the nanofibers. With the increase in aspirin concentration, the fiber diameter decreased to 80 nm from 210 nm because the charge on the surface of the jet flow increased. The aspirin that was released from fibers was observed spectrophotometrically at 270 nm. In vitro drug release studies illustrated that the highest concentration of poly(lactic acid)/silk fibroin gave the highest amount of drug release due to the bulging of fibers. When the effect on the release of aspirin content was observed, it was seen that with the increase in aspirin concentration, the amount of released drug also increased. This was due to the effect of aspirin on the diameter of the fiber mats. The

thinner are the nanofibers, the larger is the surface area and the more release of the drug from the nanofibers. The morphology of 0.7% aspirin-incorporated mats before and after its release was observed by scanning electron microscopy (SEM). Prior to the release of the drug, the morphology of nanofibers was even and drug particles were imperceptible because of their incorporation inside the nanofibers. Following drug release after 72 h, the mats swelled as a result of insolubilization (Muthumanickam et al. 2013). The appearance of the mats became rough and ruptured upon the release of aspirin, and small particles uniformly distributed on the fibers could be seen. It was concluded that after swelling, degradation of the polymer may occur and the drug may be released by diffusion and matrix erosion' (Song et al. 2012).

To check the *in vitro* blood compatibility of these composite aspirin-loaded nanofibers, a platelet adhesion experiment was carried out. The  $2 \times 2$  cm samples were fitted to the bottom of a 96-well plate and equilibrated with physiological saline for 1 h. Also, fresh human blood was added to trisodium citrate dehydrate to prevent coagulation in the ratio anticoagulant: blood of 1:9 v/v was centrifuged at 800 rpm for 10 min to get platelet-rich plasma (PRP). Following this, the nanofiber samples were incubated with 0.2 mL of PRP for 1 h at 37 °C. The samples were rinsed with phosphate-buffered saline (PBS) to eliminate loosely bound or unbound platelets. Then to prepare samples for SEM, they were fixed with 2.5% glutaraldehyde solution. After dehydration with ethanol, they were permuted with tertiary butanol and incubated in a refrigerator at 4 °C for 24 h. Lastly, the attached platelets were examined by SEM. Many adherent platelets were found attached to the pristine poly(lactic acid) nanofiber membrane. The platelets were seen to aggregate, adhere, and cover the nanofibers. Moreover, they deformed and exhibited pseudopodia. This showed the noncompatibility of pristine poly(lactic acid) nanofiber mats. On the other hand, the surface of poly(lactic acid)/silk fibroin (8/3) showed a smaller number of adhered platelets, and also fewer platelets were deformed and activated. The rationale behind the platelet adhesion on these mats was the equal proportion of hydrophilic/hydrophobic regions and the micro-phase separation in the material. Given the strong hydrophobicity of poly(lactic acid) nanofibers, poly(lactic acid)/silk fibroin nanofibers had excellent hydrophilicity/hydrophobicity balance and a good microphase separation structure. Therefore, poly(lactic acid)/silk fibroin composites had better blood compatibility. Also, some platelets attached and did not change their discoid shape on a poly(lactic acid)/silk fibroin composite having 0.9 wt.% aspirin, indicating an inactivated state. This concludes that aspirin prevented platelet stimulation and attachment and clot forming by poly(lactic acid)/silk fibroin composites.

---

### 10.3 Effect of Surface Topography of Nanofibers on Blood Compatibility

Smooth, porous, and rough nanofibers of poly(lactic acid) were fabricated in a study by electrospinning to see the effect of the topography of these nanofibers on hemocompatibility (Soundararajan et al. 2018). To prepare nanofibers with porous topography, 7% (w/v) poly(lactic acid) was dissolved in dichloromethane/acetone in

a 7:3 ratio to prepare the spinning solution. The spinning solution for smooth nanofibers was prepared by using dimethyl formamide in place of acetone in the binary solvent. Other constraints, like the concentration of polymer solutions, the magnitude of voltage, the diameter of the needle, the tip-to-collector distance, and the flow rate, were constant in both cases. To prepare nanofibers having rough topography, hydrophobic superparamagnetic iron oxide nanoparticles (SPION) were produced by coprecipitation. This SPION was complexed with curcumin to form the Cur-SPION complex. This complex (5 mg/mL) was dispersed in poly(lactic acid) polymeric solution dissolved in dichloromethane/dimethyl formamide to produce curcumin-incorporated magnetic fibers with rough topography. The water contact angle was found to be lowered in porous and rough mats as compared to the mats with smooth surfaces. The electrospun nanofibers were then analyzed for hemolysis properties. The integrity of the red blood cell membrane was analyzed by exposing the cells to different topographies of nanofibers. The human blood was incubated in 0.5 mL of 0.1 M ethylenediaminetetraacetic acid (EDTA). After centrifugation at 1500 rpm for 15 min, the pellet containing RBCs was obtained. It was followed by washing with PBS three times, and the volume was made up to 3.5 mL. Next, 0.2 mL of this suspension was pipetted out and added to 0.8 mL of distilled water set as a positive control or PBS set as a negative control. Mats were incubated in the positive control at 37 °C for 2 h, followed by centrifugation at 1500 rpm for 15 min. Then the optical density of the supernatant was measured at 540 nm, and the hemoglobin released was calculated. Following this, the hemolysis percentage was calculated. To categorize the biomaterials as hemolytic or nonhemolytic, hemolysis percentage values over 5% are taken as hemolytic. The results of the hemolysis experiment showed haptoglobin (HP) of less than 2% in smooth nanofibers (1.17%), which established the nonhemolytic behavior of smooth fibers. On the other hand, porous and rough mats showed an increased hemolysis percentage of 3.80% and 4.94%, respectively. However, this was smaller than the threshold value (hemolysis percentage >5%) (Soundararajan et al. 2018). Slight hemolysis on smooth mats can be attributed to the delicateness of RBCs on attaching to nonuniform surfaces compared to smoother surfaces. The increase in hemolysis percentage in rough nanofibers was due to the impact of surface chemistry and the rough structure on hemolysis. The efficiency of scaffolds to bind and release RBCs with no deformation was evaluated through the capture and release of RBCs. For this, 80 µL diluted RBC suspension was taken and dropped on nanofiber mats, followed by incubation for 30 min at 37 °C. To capture the cells, 2.5% glutaraldehyde was used. To release RBCs, fibers cultured with cells were first fixed with 2.5% glutaraldehyde for 1 h at 37 °C and then dehydrated with ethanol, and the fibers were imaged under FE-SEM. It was seen that porous nanofibers retained more cells than smooth nanofibers. The biconcave morphology of RBCs was also retained in both scaffolds, and adhered cells were released with 100% efficiency. In contrast, rough nanofibers (with Cur-SPION) did not have many cells attached as compared to the other two combinations. Furthermore, the anticoagulant assay was carried out to confirm the clot-inhibition properties of samples via the kinetic clotting time method. Next, 20 µL of anticoagulated blood was dispensed onto the samples and glass slabs, with the latter being taken as a positive control. Then 10 µL of CaCl<sub>2</sub> solution

(0.2 mol/L) was mixed homogeneously to induce coagulation. The samples were incubated for different time intervals of up to 60 min. Lastly, 5 mL water was added to all solutions and incubated for 5 min. Following this, the free hemoglobin in water was recorded at 540 nm. It was observed that mats with smooth, porous, and rough topographies had higher absorbance than coverslips, indicating a higher concentration of free hemoglobin and a slower rate of clotting. Furthermore, stimulated platelets were confirmed by their morphological change after adhesion to the sample surfaces from a discoid to a spread structure. Smooth fibers showed a higher number of platelets attached and had an elongated appearance with no pseudopodia formation. In contrast, porous nanofibers showed lower adhesion of platelets and retained discoidal morphology due to the hydrophilicity of fibers. The cells on Cur-SPION-modified fibers had an original discoidal shape, referring to inactivated platelets. PRT was done to assess the sample-induced time of delay in the coagulation process. Centrifugation of whole blood at 3000 rpm was performed to obtain PPP. Thereafter, tubes were incubated with nanofibers and glass coverslips (positive control) and added with 0.1–0.5 mL of PPP. From these combinations, 0.1 mL of PPP was added to 0.1 mL of  $\text{CaCl}_2$ . The time of coagulation was measured by a steel hook, which was immersed in the solution to sense fibrin threads. It was observed that the positive control activated the coagulation cascade by adsorbing the clotting proteins. On the other hand, fibers took more time for thread development than the positive control. The porous and rough nanofibers showed improved clot-inhibiting activity (234 s) compared to smooth nanofibers as they exhibited longer clotting times of 277 s and 279 s, respectively. The researchers also investigated the adsorbed serum proteins using sodium dodecyl sulfate-polyacrylamide gel electrophoresis. Samples were incubated in PRP and were allowed to adsorb for 2 h at 37 °C. The proteins that did not attach or that attached loosely were eliminated by rinsing with PBS. Then the proteins that attached to the sample surfaces were eluted using SDS. The samples were mixed with loading buffer and boiled at 95 °C for 10 min, then loaded into wells of acrylamide gel following cooling at room temperature. Electrophoresis was carried out at a voltage of 80 V in a Tris-glycine-SDS buffer. Coomassie brilliant blue dye was used to stain the adsorbed proteins after electrophoresis. It was observed that the smooth nanofibers showed high adsorption of fibronectin (200–220 kDa), prothrombin (72 kDa), and albumin (66 kDa).

---

## 10.4 Effect of Synthetic Nanofibers on Blood Compatibility

Nanofibers of polyurethane were fabricated with polyhedral oligomeric silsesquioxanes (POSS) to impart viscoelastic properties (Song et al. 2016). POSS was used due to the hollow cage assembly of silicon (Wang et al. 2009). Furthermore, it has excellent biocompatibility (Le et al. 2013; Raghunath et al. 2009). Because the hydrophobic surface with low surface energy prevent the adsorption of plasma proteins and platelets (Hasebe et al. 2013; Bhatt et al. 2011). It was assumed that incorporating POSS into polyurethane would cause a reduction in platelets and protein attachment on polyurethane mats because of lowered surface tension (Kanna



et al. 2006; Kidane et al. 2009). POSS-polyurethane spinning solutions (12%) having different concentrations of POSS (0%, 1%, and 2%) were prepared in dimethyl formamide/tetrahydrofuran (1:2). The hydrophilicity results showed that nanofibers with 2% POSS concentration had the highest water contact angle among all concentrations. The lowest contact angle was found in the case of pristine polyurethane without POSS. The reason for the increased hydrophobicity can be attributed to weak polarity due to the presence of hydrophobic POSS molecules in the polymer (Kidane et al. 2009; Teng et al. 2014). The hemolysis analysis showed that the hemolysis rate in POSS-incorporated polyurethane nanofibers reduced significantly with the increase in POSS concentration. The plasma protein adsorption assay showed a decrease in the amount of bovine serum albumin protein adsorption upon increasing POSS in the nanofibers. The adsorption amount of pristine polyurethane was  $3336.36 \mu\text{g}/\text{cm}^2$  and  $159.50 \mu\text{g}/\text{cm}^2$ , and  $115.70 \mu\text{g}/\text{cm}^2$  for the lowest and highest concentrations of POSS, respectively. Platelet adhesion was studied to analyze the hemocompatibility of nanofibers. The SEM images showed that the platelets attached more to pristine polyurethane nanofibers than to POSS-incorporated nanofibers. Furthermore, with the increase in the concentration of POSS, a smaller number of platelets got attached to the nanofiber samples. This showed the improved compatibility of samples on the incorporation of POSS. The above results of decreasing protein and platelet adsorption on POSS-incorporated polyurethane nanofibers may be ascribed to the lessening of the amount of urethanes in polyurethane on the incorporation of POSS (Groth et al. 1995). POSS also lowers the surface tension of polyurethane nanofibers, which is an advantage in inhibiting protein and platelet attachment, and lowers the binding of platelets to the nanofibers (Silver et al. 1999). After microbial culturing for 12 h, the number of *E. coli* on pristine polyurethane surfaces was the highest compared to POSS-incorporated fibers, and absolutely no growth was seen on the surface with the highest content of POSS. This indicated that the presence of POSS macromolecules could suppress bacterial growth. The reason behind the antibacterial activity of these fibers may be attributed to the lower surface tension caused by incorporating POSS in polyurethane nanofibers (Knorr et al. 2005). Also, the lotus effect of hydrophobic substrates can prevent bacterial growth due to the formation of self-cleaning surfaces (Knorr et al. 2005; Page et al. 2009; Meng et al. 2015). Furthermore, hydrophobic POSS molecule decreases the free energy of membrane and because bacteria tend to adhere to a high-energy surface (Teng et al. 2014), thereby, contributing to resist the adherence of bacteria.

A wearable artificial kidney is a new intervention for renal failure patients, replacing dialysis (Moon et al. 2017; Crews et al. 2019; Voinova et al. 2019). Studies are aiming to fabricate dialyzers by modifying membranes for blood purification through convection, diffusion, or adsorption (Castro et al. 2018; Mohammadi et al. 2018; Sultan et al. 2019). Studies have proven that zeolite is a potential material for the selective adsorption of toxins in an artificial kidney (Narasimhan et al. 2013; Arstad et al. 2008). The powder form of zeolite is unfit for use in dialysis due to its loose powder-like appearance. Therefore, some hydrophilic and biocompatible materials need to be used as substrates. Poly(vinyl pyrrolidone) due to its excellent

biocompatibility, and solubility in organic and inorganic solvents. This polymer has good spinnability when the electric field is applied and has been used in engineering materials (Huang et al. 2016). It is potentially apt to use along with zeolites and acts as an adhesive for binding zeolite nanoparticles. However, due to the poor mechanical strength of poly(vinyl pyrrolidone), polyether sulfone polymers are the better choice for dialysis membranes because of their desirable characteristics (Qu et al. 2010). So, in this regard, a wearable blood purification system was proposed (Haghdoust et al. 2021). In this study, polyether sulfone/poly(vinyl pyrrolidone)-zeolite was fabricated by single-step electrospinning. Core spinning was employed with polyether sulfone solution and shell spinning with poly(vinyl pyrrolidone)-incorporated zeolites. Poly(vinyl pyrrolidone) prevented zeolites from discharging into circulation. Two types of zeolites were used in their study, viz., CP8C11 (beta) and ZSM-5 zeolites, due to their ability to attach creatinine from the solution. Polyether sulfone spinning solution (25% v/v) was prepared in dimethyl formamide. Poly(vinyl pyrrolidone)/zeolite solution was prepared by dissolving (10% v/v) in binary solvent dimethyl formamide: acetone. Following this, ZSM-5 and other beta zeolites (10% and 20%) were added to the poly(vinyl pyrrolidone) solution. It was observed that the beta zeolites adsorbed the creatinine more than the ZSM-5 zeolites. Also, the silicon/aluminum ratio is an aspect of creatinine adherence (Lu et al. 2017; Namekawa et al. 2014). It is shown in Fig. 10.3 that the adsorption capacity of beta zeolite decreases with an increase in its concentration due to zeolite aggregation at high concentrations, which in turn lowers the surface area for adsorption.

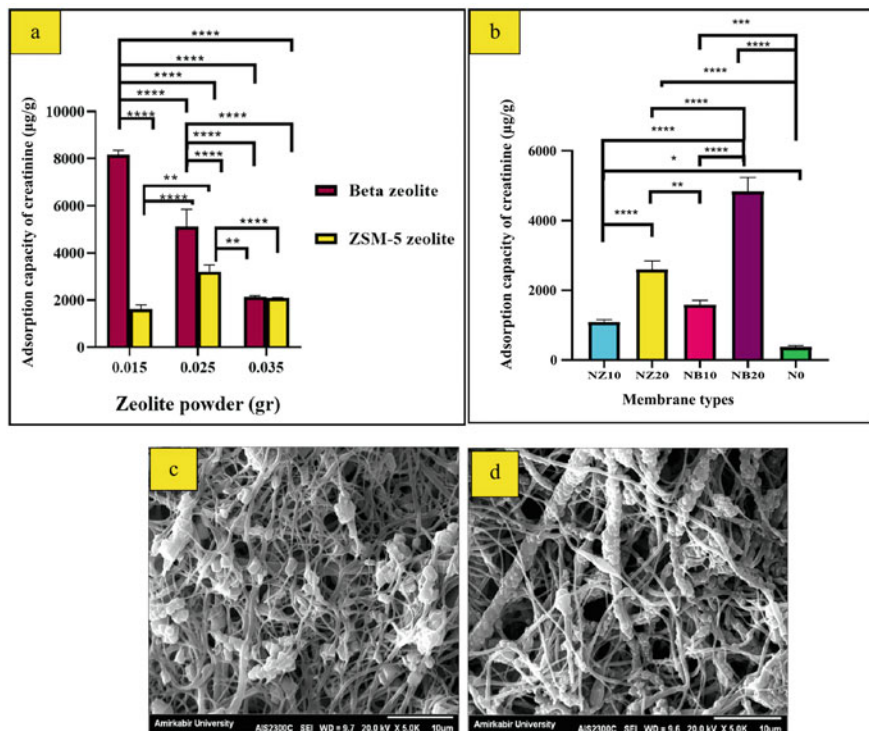
The cytotoxicity of polyether sulfone/poly(vinyl pyrrolidone)-zeolite nanofibers was investigated. Figure 10.4 shows the cell viability results of commercial polyether sulfone, the core-shell nanofiber of polyether sulfone/poly(vinyl pyrrolidone), and zeolite-incorporated polyether sulfone/poly(vinyl pyrrolidone) nanofiber. The growth of fibroblasts on the core-shell nanofibers was as desired till 24 h. This study suggested the efficient use of core-shell nanofibers (viability of over 90%) for blood purification in dialysis approaches. Moreover, the optical microscope images are shown in Fig. 10.5 to observe the viability of fibroblasts after 24 and 48 h of cell culture with samples.

Figure 10.6 shows the platelet adhesion results of the samples. No pseudopod morphology was acquired by cells on the samples, which indicates no platelet stimulation and good compatibility of zeolites. These images (Fig. 10.6) illustrate none of the adsorbed platelets on zeolite-incorporated nanofibers. However, there was a significant number of platelets attached to pure nanofibers.

---

## 10.5 Effect of Natural Nanofibers on Blood Compatibility

Carboxymethyl chitosan is a widely used derivative of chitosan used in biomaterial fabrication. Its compatibility with the blood system has been reported in the literature (Fu et al. 2011). Moreover, it is used in modifying other polymers also to improve blood compatibility (Aiping and Tian 2006). Electrospun carboxymethyl chitosan and poly(lactic acid) nanofibers were prepared to test their compatibility with blood



**Fig. 10.3** (a) Solution adsorption capacity of creatinine using zeolite (powder type), (b) creatinine adsorption by core-shell nanofiber (membrane type), (c) micrographs of creatinine solution adsorption of ZSM-5 zeolite 20% incorporated polyether sulfone/poly(vinyl pyrrolidone) nanofibers, and (d) micrographs of creatinine solution adsorption of beta zeolite 20% incorporated polyether sulfone/poly(vinyl pyrrolidone) nanofibers. (Reproduced with permission from Haghdoost et al. 2021)

(Lv et al. 2017). Carboxymethyl chitosan nanopowder was prepared by ball milling from 400 mg carboxymethyl chitosan powder. Carboxymethyl chitosan was downsized by two steel balls with a 5 mm radius for 4 h at 20 Hz, and carboxymethyl chitosan nanopowder was obtained. To prepare the spinning solution, 8% poly(lactic acid) prepared in binary solvent dimethyl formamide and dichloromethane ( $v/v = 7/3$ ) was mixed with 400 mg carboxymethyl chitosan nanopowder under constant magnetic stirring. The carboxymethyl chitosan/poly(lactic acid) membranes were linked in 50% glutaraldehyde solution at 80 °C for 12 h, followed by 0.1 mol/L glycine treatment to block unreacted aldehyde groups.

Multilayered silk fibroin was obtained from tussah cocoons incorporated in poly(lactic acid) nanofibers by electrospinning (Shao et al. 2017). The silk fibroin sponge was prepared following the treatment of cocoons, viz., degumming, dissolving, dialysis, and lyophilization. Next, the silk fibroin sponge and poly(lactic acid) were dissolved in 1,1,1,3,3,3-hexafluoro-2-propanol in different proportions to

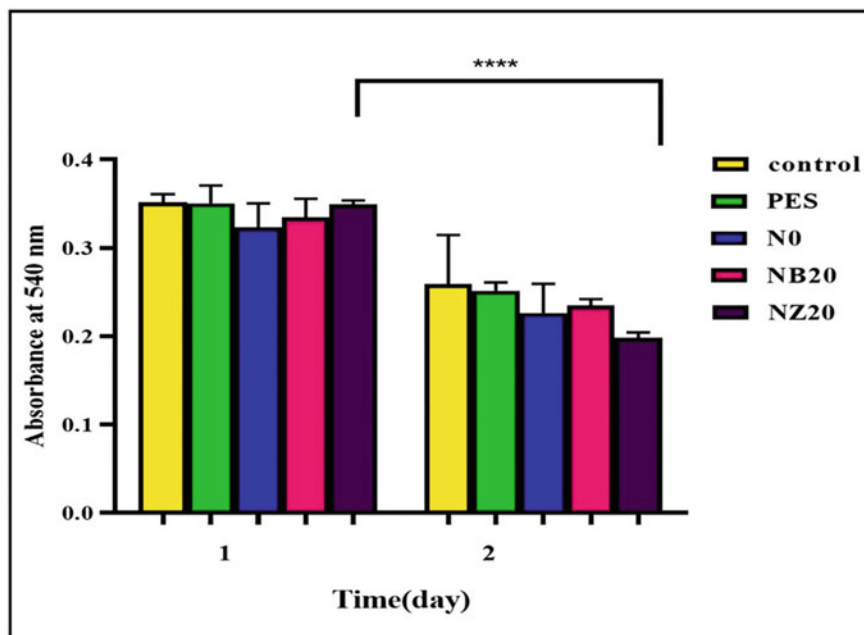


**Fig. 10.4** Cell viability results at 540 nm absorbance of nanofibers with different zeolite concentrations, where control is the tissue culture plate, PES is pristine polyether sulfone nanofiber, N0 is pristine polyether sulfone/poly(vinyl pyrrolidone) nanofiber, NB20 is 20% beta zeolite, and NZ20 is 20% ZSM-5 zeolite. (Reproduced from Haghdoost et al. 2021)

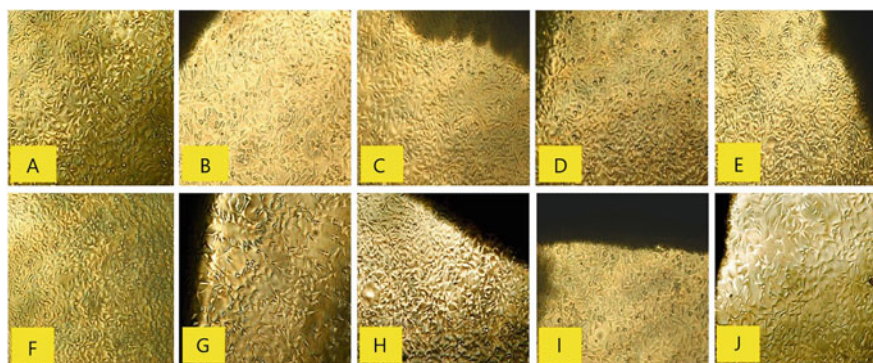


**Fig. 10.5** Optical microscope images showing the proliferation of fibroblasts (a) and (f) tissue culture plate; (b) and (g) polyether sulfone; (c) and (h) pure; (d) and (i) NZ20; (e) and (j) NB20. Top (after 24 h) and bottom (after 48 h). (Reproduced with permission from Haghdoost et al. 2021)

make the final concentration of the spinning solution 8%. To prepare the nanofiber mats, the nanofiber yarns were electrospun, and a fiber web was formed by rotating them in a funnel. To fabricate multilayer fibers, parallel twisted and weft strands of these yarns were intertwined longitudinally to produce a fabric sheet. Three layers

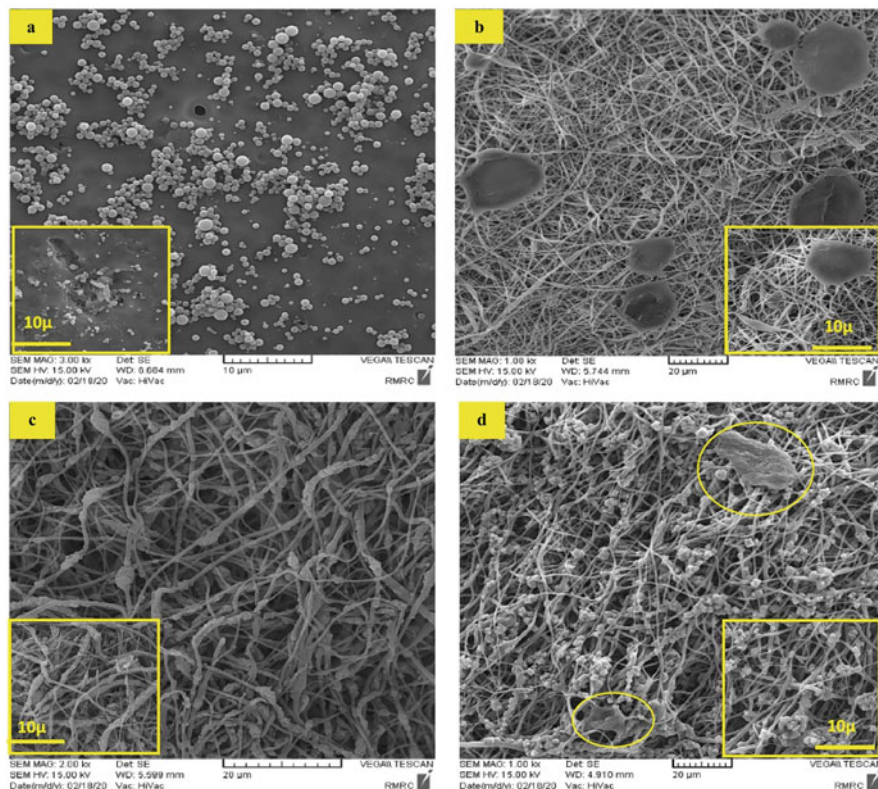


**Fig. 10.6** SEM micrographs of platelet attachment on (a) commercial polyether sulfone, (b) pure polyether sulfone/poly(vinyl pyrrolidone), (c) beta-zeolite-incorporated nanofibers, (d) Z20-incorporated nanofibers. (Reproduced with permission from Haghdoost et al. 2021)

were later combined with seriatim, and a multilayered nanofiber fabric membrane was formed. To test for biomineralization, simulated body fluid was prepared, and 1% of aspartic acid (a polymer that dissolves in aqueous solvents) was mixed to bring about mineralization. The electrospun nanofiber mats were soaked in simulated body fluid and kept at 37 °C for 72 h, and the medium was replaced every day. Following this, samples were washed with distilled water and deposited on coverslips after freeze-drying. Following mineralization, the samples were observed under SEM after 6, 12, 24, and 72 h (Fig. 10.7). At 6 h, the surface of the samples showed little mineralization in addition to discontinuous mineral clusters; at some points, these particles were observed until mineralization time of 24 h. The reason may be the hydrophobic nature of the poly(lactic acid) surface, which cannot easily constrain the calcium present in simulated body fluid in the form of ions and nucleation points. The surface of multilayer poly(lactic acid)/silk fibroin nanofibers showed a higher number of spherical particles at 6 h as compared to pure poly(lactic acid). After 12 h, the mineral particles covered about all of the nanofibers,

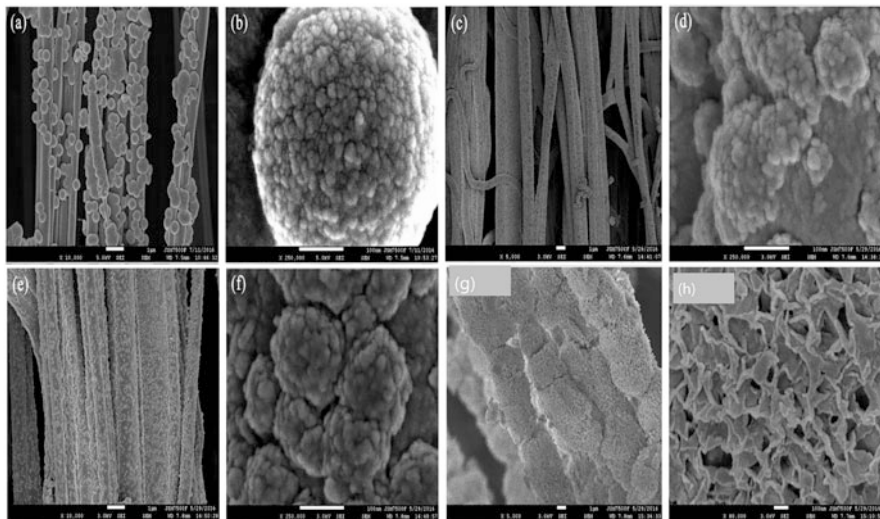


**Fig. 10.7** SEM micrographs of silk fibroin and poly(lactic acid) nanofibers after biom mineralization for different time intervals: (a, b) 6 h; (c, d) 12 h; (e, f) 24 h; (g, h) 72 h. (Reproduced with permission from Shao et al. 2017)

with a decrease in their diameter. At 24 h of mineralization, the particles further reduced in diameter and got compressed together to cover all nanofibers.

Nanofiber mats were placed in a 24-well tissue culture plate, treated with PBS for 2 h, and then added with 75% ethanol for sterilization. Following this, the fibers were incubated for 24 h at 37 °C in the presence of 1 mL of 10% fetal bovine serum. The absorbance was measured at 280 nm to check the concentration of fetal bovine serum proteins prior to and after adsorption. The blood compatibility was quantified by hemolysis assay, and the hemolysis rate was measured in all cases. The poly(lactic acid)/silk fibroin mats had a hemolysis rate of 0.9%, indicating their good blood compatibility. The proliferation of cells cultured on poly(lactic acid)/silk fibroin/hyaluronic acid multilayered mats was found to be enormously higher than on poly(lactic acid)/silk fibroin. It was also found that the proliferation on reference coverslips was low, pointing out that the mineral crystals on the nanofibers promote proliferation. Both nanofiber mats and nanofiber fabrics showed the same value on day 4 of cell culture. On the other hand, the proliferation on fabrics was a bit increased compared to the fiber mats on day 7. The morphology of mesenchymal stem cells (MSCs) was determined by confocal laser scanning microscopy (Fig. 10.8). A directional growth of cells was seen on the nanofiber fabric along the axial direction of the yarn; however, the cells on nanofiber mats showed a random arrangement. This phenomenon might arise due to the contact guidance of the underlying substrate, such as nanopatterned material and nanofiber (Laco et al. 2013). Also, the fluorescence intensity on the fabric group was higher compared to mats with multilayered nanofiber fabrics, which offer a much optimal environment for the proliferation of cells.

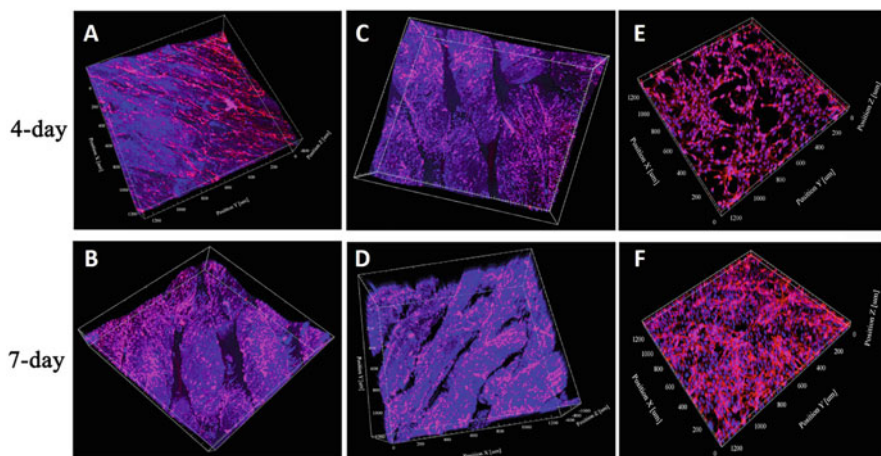


**Fig. 10.8** The confocal microscope images of MSCs grown on (a and b) poly(lactic acid)/silk fibroin fabric, (c and d) poly(lactic acid)/silk fibroin/hyaluronic acid fabric, and (e and f) poly(lactic acid)/silk fibroin/hyaluronic acid mats at 4 and 7 days of culture. (Reproduced with permission from Shao et al. 2017)

The expression of marker genes on cells attached to the mats for different times (7, 14, and 21 days) was analyzed. After culture, the cells were washed with PBS and suspended in a cold TRIzol reagent. cDNA was produced using the first-strand synthesis system, which was later on followed by quantitative PCR using SYBR Green. The marker genes for osteocytes that were used were those for alkaline phosphatase (ALP), osteocalcin (OCN), osteopontin (OPN), and collagen type I (Col I). After 14 days, ALP and type I collagen expression levels were much higher in all nanofiber groups (Fig. 10.9a, b). The mineralization of nanofibers increased the osteogenic differentiation of MSCs. After 21 days of culture, the OCN gene (a marker for the late expression of osteogenesis) expression in cells increased by threefolds on poly(lactic acid)/silk fibroin/hyaluronic acid nanofiber mats than on the poly(lactic acid)/silk fibroin group, which indicated that hyaluronic acid accelerated the differentiation of osteoblasts (Fig. 10.9c). In addition to this, OPN gene expression in cells cultured on fabric scaffolds had higher levels of expression than on nanofiber scaffolds after 7 days of culture (Fig. 10.9d), indicating that the arrangement of nanofibers can promote the differentiation of MSCs into osteoblasts.

## 10.6 Effect of Growth-Factor-Incorporated Nanofibers on Blood Compatibility

Vascular grafts made from polymeric nanofibers have been used in treating vascular diseases (Desai et al. 2011). However, these grafts should prevent platelet aggregation and promote endothelialization on the surface of the graft. To achieve this goal, many bioactive molecules have been merged in the grafts to modify their characters.

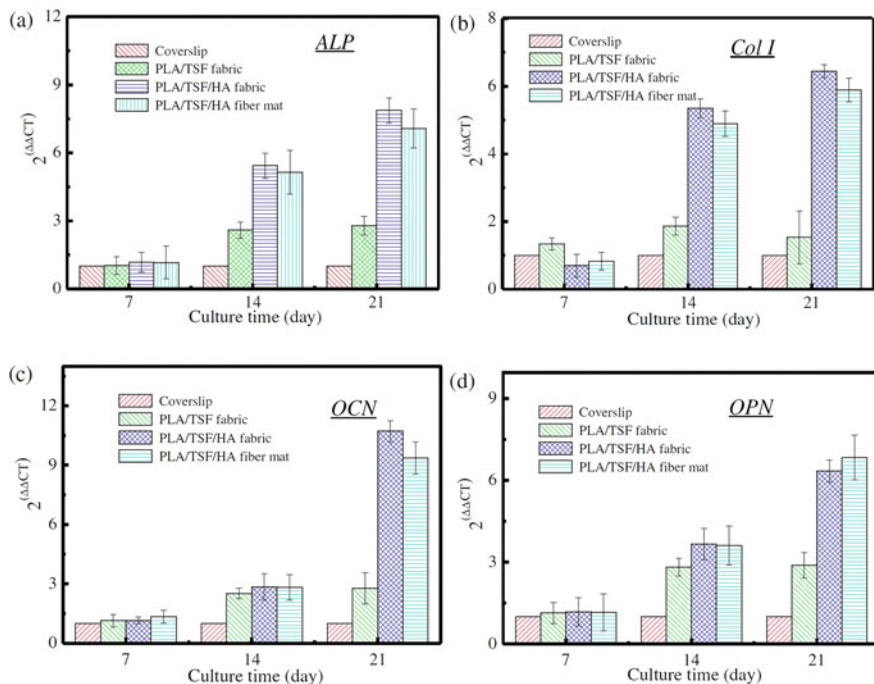


**Fig. 10.9** The expression of genes obtained from RT-PCR: (a) alkaline phosphatase, (b) collagen type I, (c) osteocalcin, (d) osteopontin. (Reproduced with permission from Shao et al. 2017)

For instance, anticoagulant heparin has been routinely introduced into tissue materials to inhibit thrombogenesis (Hoshi et al. 2013; Yao et al. 2014; Seib et al. 2014). Furthermore, vascular endothelial growth factor (VEGF) is also an effective molecule for endothelialization (Coultas et al. 2005; Asahara et al. 1999). Despite the benefits of VEGF in endothelial progenitor cell (EPC) proliferation (Asahara et al. 1999), it has a rapid half-life in the biological system (Takeshita et al. 1994). Therefore, any delivery agent used for VEGF should preserve its activity and release it at a precise rate. Given this, diverse quantities of heparin were encapsulated into a poly(L-lactic acid-co-ε-caprolactone) nanofiber through emulsion electrospinning, followed by hemocompatibility analysis (Chen et al. 2015). Furthermore, the optimal concentration of heparin was selected and encapsulated, along with VEGF, to form nanofibers. For spinning solutions, aqueous solutions of heparin in distilled water with varying concentrations (5%, 10%, and 15%) were prepared. The internal structure of the nanofibers was examined with transmission electron microscopy (TEM). For this, the samples were prepared by directly depositing fibers on copper grids. The TEM images showed that the composite poly(L-lactic acid-co-ε-caprolactone) scaffolds presumed a uniform core-shell morphology (Fig. 10.10a, b). However, the fibers with heparin and those with or without VEGF had a no-uniform multicore shell conformation, and the incorporated factors



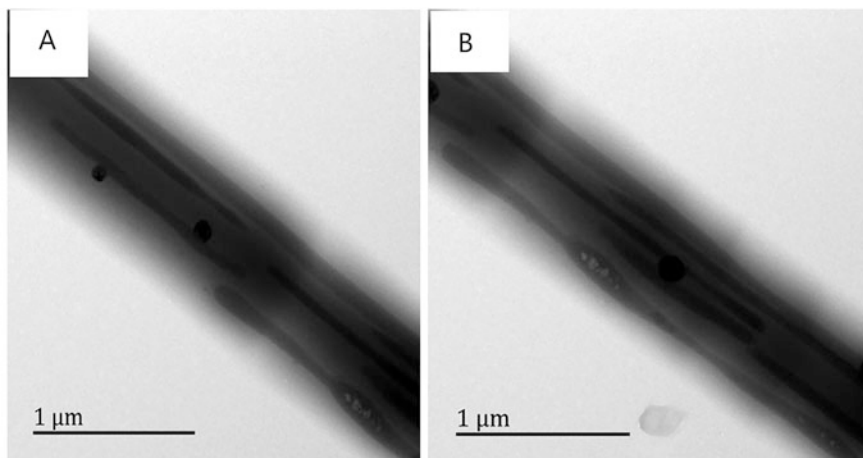


**Fig. 10.10** TEM images of different electrospun poly(L-lactic acid-co- $\epsilon$ -caprolactone) nanofibers, (a) Poly(L-lactic acid-co- $\epsilon$ -caprolactone) incorporated heparin; (b) Poly(L-lactic acid-co- $\epsilon$ -caprolactone) incorporated heparin and VEGF. (Reproduced with permission from Chen et al. 2015)

showed a zonal distribution inside the fibers. The reason for this is that heparin, because of its strong negative charge, increased interdroplet repulsion, leading to the discontinuous core-shell morphology at the time of stretching and evaporation.

The optimum release of heparin and VEGF from the nanofibers was recorded. The poly(L-lactic acid-co- $\epsilon$ -caprolactone) scaffolds containing varied concentrations of heparin and VEGF were immersed in 5 mL of PBS solution and incubated. At different time intervals, 1 mL of the supernatant was pipetted out, and 1 mL of fresh medium was added. To measure the release of heparin from nanofibers, a toluidine blue test was conducted, and to measure VEGF release, an enzyme-linked immunosorbent assay kit was used. The release profiles of heparin and VEGF showed two stages. There was a constant release of heparin for 6 days; after this, a slow release was observed for 29 days. However, there was no perceptible change between the scheme for the release of heparin in the two different concentrations of composite nanofibers, which indicated that VEGF has no role in the release of heparin. On the other hand, the release profile of VEGF was different compared to that of heparin. Due to the higher amount of heparin than of VEGF, the release of VEGF was significantly affected. VEGF release was higher from both types of scaffolds until day 4, which was followed by a slow and constant release. In the scaffold with a higher concentration of VEGF (20%), more VEGF was released compared to the scaffold with 15% VEGF. The results indicate that the amount of VEGF release significantly depends on the loading amount of heparin and that both the growth factors loaded in fibers can be released in a tuned style (Fig. 10.11).

The hemolysis assay revealed hemolysis rates of less than 5%, indicating good blood compatibility of all mats. The hemolysis rate for poly(L-lactic acid-co- $\epsilon$ -caprolactone) with 10% heparin and 15% heparin were less than 0, indicating

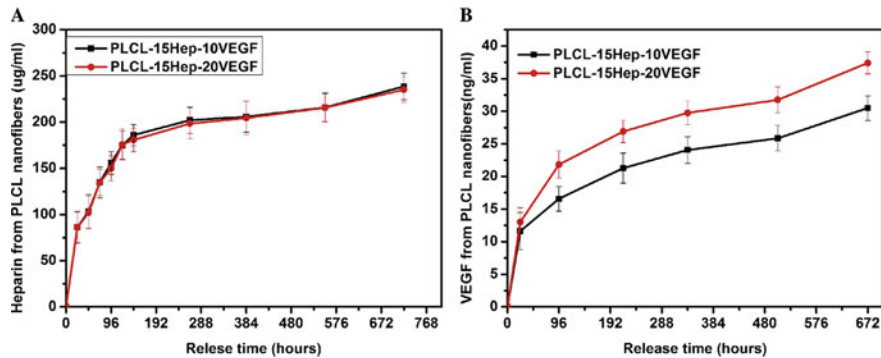


**Fig. 10.11** Release profiles of heparin (a) and VEGF (b) from different poly(L-lactic acid-co- $\epsilon$ -caprolactone) (PLCL) mats. (Reproduced with permission from Chen et al. 2015)

very few ruptured RBCs than the negative control. The reason for this may be attributed to the anticoagulant properties of heparin and also because it acts as a regulator of the complement system (Ninomiya et al. 2000). It has also been studied that heparin has an important role in the regulation of complement-system-induced hemolysis (Mannari et al. 2008). The platelet adhesion studies showed that the number of platelets that adhered to the nanofibers with loaded heparin was lesser as compared to the pure poly(L-lactic acid-co- $\epsilon$ -caprolactone). For the biocompatibility assay, bone marrow cells were produced from the bones of Sprague-Dawley rats (weight = 200–250 g). The mononuclear cells having low density were separated by density gradient centrifugation in a medium exclusive for lymphocytes. The detached cells were resuspended in a culture medium (EGM-2), having the optimal composition for the lymphocytes to grow. Lastly, mononuclear cells were seeded on fibronectin-coated plates and incubated with ample  $\text{CO}_2$  supply at a temperature of 37 °C. Fluorescence microscopy confirmed the presence of endothelial progenitor cells (EPCs) by imaging double-positive cells. Furthermore, fluorescence-activated cell sorting (FACS) confirmed the EPCs characteristics of cells by confirming the presence of CD34 and VEGFR-2(KDR) in cells. Cell growth was recorded by a cell counting kit-8 (CCK-8) assay. The samples were placed at the bottom of 24-well plates, and cells were seeded and grown for different time intervals for 7 days. CCK-8 solution was added to the wells already containing the culture medium at a concentration of 10  $\mu\text{L}/100 \mu\text{L}$ , and the samples were raised for 2 h in this solution. Following this, absorbance was measured at 490 nm. Cell viability was determined by correlating the amount of absorbance with the number of viable cells. In addition to this, two more plates were cultured for 7 days. One plate was set for the fluorescent staining to determine the morphology and quantity of cells and the other for SEM to see the cell attachment on the surface of scaffolds. Absorbance was noticeably higher in VEGF-incorporated fibers than in pure fibers (Fig. 10.12). The results suggest that EPCs multiply faster on VEGF-incorporated fibers than those without VEGF, and this effect was concentration and time-dependent.

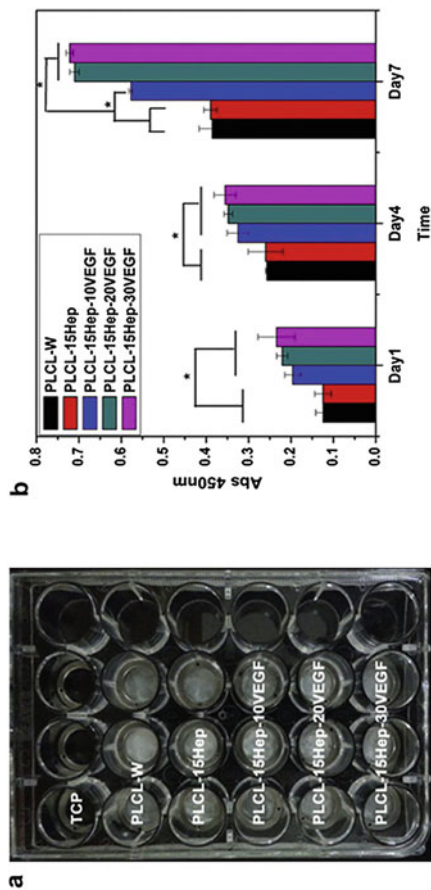


**Fig. 10.12** (a) Image of the 24-well plate showing the distribution of five types of scaffold samples. (b) The CCK-8 assay for the viability of EPCs on five types of poly(L-lactic acid-co-ε-caprolactone) nanofiber mats. (Reproduced with permission from Chen et al. 2015)

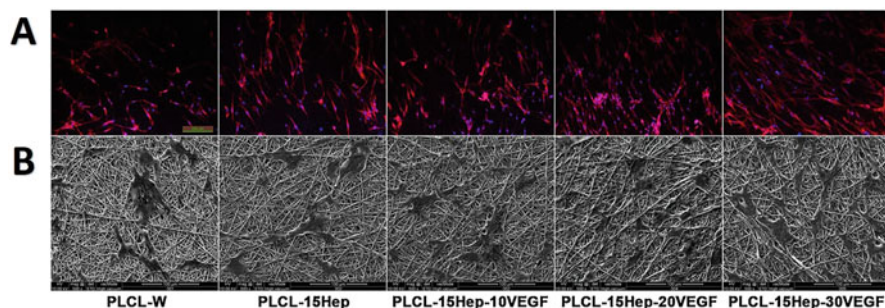


**Fig. 10.13** (a) Immunofluorescent images of EPCs cultured on composite poly(L-lactic acid-co-ε-caprolactone) nanofibers. (b) SEM images of the EPCs attached on nanofibers show proliferation. (Reproduced with permission from Chen et al. 2015)

The structure and number of cells were revealed by immunofluorescence staining, shown in Fig. 10.13a, b. The morphology of cells and their interaction with nanofibers were analyzed by SEM. After 7 days of culture, the cells spread well on the nanofiber surfaces incorporated with VEGF.

---

## 10.7 Conclusion

In this chapter, the impact of different agents when incorporated into nanofiber has been discussed, which in turn reflects blood compatibility. The different assays for testing hemocompatibility have also been discussed in detail. We also discussed how different topographies of the nanofibers could impact the blood compatibility of a nanofiber sample. It was also seen that the introduction of growth factors and drugs causes variation in blood compatibility. For example, aspirin loading showed an enhanced effect of the anticoagulation of the poly(lactic acid)/silk fibroin nanofibers. Furthermore, the method of fabrication of nanofibers and the choice of polymer can significantly influence hemocompatibility. In conclusion, the chapter gives information on the biocompatible properties of different nanofibers and their use in other biomedical applications.

**Acknowledgments** This work was supported by the Science and Engineering Research Board (SERB) research grants (CRG/2020/000113) and Council of Scientific & Industrial Research (CSIR) (File No: 22(0846)/20/EMR-II) research grants.

---

## References

Aiping Z, Tian C (2006) Blood compatibility of surface-engineered poly (ethylene terephthalate) via o-carboxymethylchitosan. *Colloids Surf B Biointerfaces* 50(2):120–125. <https://www.sciencedirect.com/science/article/pii/S0927776506001536>. Accessed 5 Sep 2022

- Arstad B, Fjellvåg H, Kongshaug KO, Swang O, Blom R (2008) Amine functionalised metal organic frameworks (MOFs) as adsorbents for carbon dioxide. *Adsorption* 14(6):755–762. <https://doi.org/10.1007/s10450-008-9137-6>
- Asahara T et al (1999) VEGF contributes to postnatal neovascularization by mobilizing bone marrow-derived endothelial progenitor cells. *EMBO J* 18(14):3964–3972. <https://doi.org/10.1093/emboj/18.14.3964>
- Balan V, Verestiuc L (2014) Strategies to improve chitosan hemocompatibility: a review. *Eur Polym J* 53(1):171–188. <https://doi.org/10.1016/j.eurpolymj.2014.01.033>
- Bhatt S et al (2011) Nanostructure protein repellent amphiphilic copolymer coatings with optimized surface energy by inductively excited low pressure plasma. *Langmuir* 27(23):14570–14580. <https://doi.org/10.1021/la203256w>
- Castro AC, Neri M, Nayak Karopadi A, Lorenzin A, Marchionna N, Ronco C (2018) Wearable artificial kidney and wearable ultrafiltration device vascular access - future directions. *Clin Kidney J* 12(2):300–307. <https://doi.org/10.1093/ckj/sfy086>
- Chen L, Han D, Jiang L (2011) On improving blood compatibility: from bioinspired to synthetic design and fabrication of biointerfacial topography at micro/nano scales. *Colloids Surf B Biointerfaces* 85(1):2–7. <https://doi.org/10.1016/j.colsurfb.2010.10.034>
- Chen X et al (2015) Electrospun poly(l-lactic acid-co-ε-caprolactone) fibers loaded with heparin and vascular endothelial growth factor to improve blood compatibility and endothelial progenitor cell proliferation. *Colloids Surf B Biointerfaces* 128:106–114. <https://doi.org/10.1016/j.colsurfb.2015.02.023>
- Coultas L, Chawengsaksophak K, Rossant J (2005) Endothelial cells and VEGF in vascular development. *Nature* 438(7070):937–945. <https://doi.org/10.1038/nature04479>
- Crews DC, Bello AK, Saadi G (2019) 2019 World Kidney Day Editorial - Burden, access, and disparities in kidney disease. *Jornal brasileiro de nefrologia* 41(1):1–9. <https://doi.org/10.1590/2175-8239-JBN-2018-0224>
- Dash M, Chiellini F, Ottenbrite RM, Chiellini E (2011) Chitosan - a versatile semi-synthetic polymer in biomedical applications. *Prog Polym Sci (Oxford)* 36(8):981–1014. <https://doi.org/10.1016/j.progpolymsci.2011.02.001>
- De Mel A, Cousins BG, Seifalian AM (2012) Surface modification of biomaterials: a quest for blood compatibility. *Int J Biomater*. <https://doi.org/10.1155/2012/707863>
- Denis FA et al (2002) Protein adsorption on model surfaces with controlled nanotopography and chemistry. *Langmuir* 18(3):819–828. <https://doi.org/10.1021/la011011o>
- Desai M, Seifalian AM, Hamilton G (2011) Role of prosthetic conduits in coronary artery bypass grafting. *Eur J Cardiothorac Surg* 40(2):394–398. <https://doi.org/10.1016/j.ejcts.2010.11.050>
- Dev A et al (2010) Preparation of poly(lactic acid)/chitosan nanoparticles for anti-HIV drug delivery applications. *Carbohydr Polym* 80(3):833–838. <https://doi.org/10.1016/j.carbpol.2009.12.040>
- Fei Y, Chen Y, Wang H, Gao W, Yang R, Wan Y (2011) Preparation, characterization of antibacterial PLA/TP nanofibers. *Fibers Polym* 12(3):340–344. <https://doi.org/10.1007/s12221-011-0340-9>
- Freitas SC, Barbosa MA, Martins MCL (2010) The effect of immobilization of thrombin inhibitors onto self-assembled monolayers on the adsorption and activity of thrombin. *Biomaterials* 31(14):3772–3780. <https://doi.org/10.1016/j.biomaterials.2010.01.097>
- Fu D, Han B, Dong W, Yang Z, Lv Y, Liu W (2011) Effects of carboxymethyl chitosan on the blood system of rats. *Biochem Biophys Res Commun* 408(1):110–114. <https://doi.org/10.1016/j.bbrc.2011.03.130>
- Gorbet MB, Sefton MV (2006) Biomaterial-associated thrombosis: roles of coagulation factors, complement, platelets and leukocytes. In: *The biomaterials: Silver Jubilee Compendium*, pp 219–241
- Groth T, Campbell EJ, Herrmann K, Seifert B (1995) Application of enzyme immunoassays for testing haemocompatibility of biomedical polymers. *Biomaterials* 16(13):1009–1015. [https://doi.org/10.1016/0142-9612\(95\)94909-5](https://doi.org/10.1016/0142-9612(95)94909-5)

- Haghdoust F, Bahrami SH, Barzin J, Ghaee A (2021) Preparation and characterization of electrospun polyethersulfone/polyvinylpyrrolidone-zeolite core-shell composite nanofibers for creatinine adsorption. *Sep Purif Technol* 257:117881. <https://doi.org/10.1016/j.seppur.2020.117881>
- Hasebe T et al (2013) Hydrophobicity and non-thrombogenicity of nanoscale dual rough surface coated with fluorine-incorporated diamond-like carbon films: biomimetic surface for blood-contacting medical devices. *Diam Relat Mater* 38:14–18. <https://doi.org/10.1016/j.diamond.2013.06.001>
- Hauert R (2005) A review of DLC coatings for biological applications. *Proc World Tribol Congress III 2005*:681–682. <https://doi.org/10.1115/wtc2005-63879>
- He C et al (2011) Chemically induced graft copolymerization of 2-hydroxyethyl methacrylate onto polyurethane surface for improving blood compatibility. *Appl Surf Sci* 258(2):755–760. <https://doi.org/10.1016/j.apsusc.2011.08.074>
- Hoshi RA, Van Lith R, Jen MC, Allen JB, Lapidus KA, Ameer G (2013) The blood and vascular cell compatibility of heparin-modified ePTFE vascular grafts. *Biomaterials* 34(1):30–41. <https://doi.org/10.1016/j.biomaterials.2012.09.046>
- Hou C, Yuan Q, Huo D, Zheng S, Zhan D (2008) Investigation on clotting and hemolysis characteristics of heparin-immobilized polyether sulfones biomembrane. *J Biomed Mater Res A* 85(3):847–852. <https://doi.org/10.1002/jbm.a.31502>
- Hsiao CR, Lin CW, Chou CM, Chung CJ, He JL (2015) Surface modification of blood-contacting biomaterials by plasma-polymerized superhydrophobic films using hexamethyldisiloxane and tetrafluoromethane as precursors. *Appl Surf Sci* 346:50–56. <https://doi.org/10.1016/j.apsusc.2015.03.208>
- Huang XJ, Guduru D, Xu ZK, Vienken J, Groth T (2011) Blood compatibility and permeability of heparin-modified polysulfone as potential membrane for simultaneous hemodialysis and LDL removal. *Macromol Biosci* 11(1):131–140. <https://doi.org/10.1002/mabi.201000278>
- Huang S, Zhou L, Li MC, Wu Q, Kojima Y, Zhou D (2016) Preparation and properties of electrospun poly(vinyl pyrrolidone)/cellulose nanocrystal/silver nanoparticle composite fibers. *Materials (Basel)* 9:7. <https://doi.org/10.3390/ma9070523>
- Kanna RY et al (2006) The antithrombogenic potential of a polyhedral oligomeric silsesquioxane (POSS) nanocomposite. *Biomacromolecules* 7(1):215–223. <https://doi.org/10.1021/bm050590z>
- Kidane AG, Burriesci G, Edirisinghe M, Ghanbari H, Bonhoeffer P, Seifalian AM (2009) A novel nanocomposite polymer for development of synthetic heart valve leaflets. *Acta Biomater* 5(7): 2409–2417. <https://doi.org/10.1016/j.actbio.2009.02.025>
- Kim JH, Kim SC (2002) PEO-grafting on PU/PS IPNs for enhanced blood compatibility - effect of pendant length and grafting density. *Biomaterials* 23(9):2015–2025. [https://doi.org/10.1016/S0142-9612\(01\)00330-1](https://doi.org/10.1016/S0142-9612(01)00330-1)
- Kim ES, Kim SH, Lee CH (2010) Electrospinning of polylactide fibers containing silver nanoparticles. *Macromol Res* 18(3):215–221. <https://doi.org/10.1007/s13233-010-0316-4>
- Knorr SD, Combe EC, Wolff LF, Hodges JS (2005) The surface free energy of dental gold-based materials. *Dent Mater* 21(3):272–277. <https://doi.org/10.1016/j.dental.2004.06.002>
- Kurakula M, Koteswara Rao GSN (2020) Moving polyvinyl pyrrolidone electrospun nanofibers and bioprinted scaffolds toward multidisciplinary biomedical applications. *Eur Polym J* 136: 109919. <https://doi.org/10.1016/j.eurpolymj.2020.109919>
- Laco F, Grant MH, Black RA (2013) Collagen-nanofiber hydrogel composites promote contact guidance of human lymphatic microvascular endothelial cells and directed capillary tube formation. *J Biomed Mater Res A* 101A(6):1787–1799. <https://doi.org/10.1002/jbm.a.34468>
- Le X, Poinern G, Ali N et al (2013) Engineering a biocompatible scaffold with either micrometre or nanometre scale surface topography for promoting protein adsorption and cellular response. [hindawi.com](https://www.hindawi.com). <https://www.hindawi.com/journals/ijbm/2013/782549/>. Accessed 5 Sept 2022
- Leszczak V, Smith BS, Popat KC (2013) Hemocompatibility of polymeric nanostructured surfaces. *J Biomater Sci Polym Ed* 24(13):1529–1548. <https://doi.org/10.1080/09205063.2013.777228>

- Li Q, Dunn ET, Grandmaison EW, Goosen MFA (1992) Applications and properties of chitosan. *J Bioact Compat Polym* 7(4):370–397. <https://doi.org/10.1177/088391159200700406>
- Li L et al (2011) Electrospun poly( $\epsilon$ -caprolactone)/silk fibroin core-sheath nanofibers and their potential applications in tissue engineering and drug release. *Int J Biol Macromol* 49(2): 223–232. <https://doi.org/10.1016/j.ijbiomac.2011.04.018>
- Lluch C, Lligadas G, Ronda JC, Galà M, Cádiz V (2013) Thermoplastic polyurethanes from undecylenic acid-based soft segments: structural features and release properties. *Macromol Biosci* 13(5):614–622. <https://doi.org/10.1002/mabi.201200433>
- Lu L, Chen C, Samarasekera C, Yeow JTW (2017) Influence of zeolite shape and particle size on their capacity to adsorb uremic toxin as powders and as fillers in membranes. *J Biomed Mater Res B Appl Biomater* 105(6):1594–1601. <https://doi.org/10.1002/jbm.b.33698>
- Lv J, Yin X, Zeng Q, Dong W, Liu H, Zhu L (2017) Preparation of carboxymethyl chitosan nanofibers through electrospinning the ball-milled nanopowders with poly(lactic acid) and the blood compatibility of the electrospun NCMC/PLA mats. *J Polym Res* 24(4):60. <https://doi.org/10.1007/s10965-017-1224-5>
- Mannari D, Liu C, Hughes D, Mehta A (2008) The role of heparin in alleviating complement-mediated acute intravascular haemolysis. *Acta Haematol* 119(3):166–168. <https://doi.org/10.1159/000134221>
- Meng J et al (2015) Antibacterial cellulose membrane via one-step covalent immobilization of ammonium/amine groups. *Desalination* 359:156–166. <https://doi.org/10.1016/j.desal.2014.12.032>
- Mohammadi F, Valipouri A, Semnani D, Alsahebhosoul F (2018) Nanofibrous tubular membrane for blood hemodialysis. *Appl Biochem Biotechnol* 186(2):443–458. <https://doi.org/10.1007/s12010-018-2744-0>
- Moon BM et al (2017) Novel fabrication method of the peritoneal dialysis filter using silk fibroin with urease fixation system. *J Biomed Mater Res B Appl Biomater* 105(7):2136–2144. <https://doi.org/10.1002/jbm.b.33751>
- Muthumanickam A, Subramanian S, Goweri M, Sofi Beaula W, Ganesh V (2013) Comparative study on eri silk and mulberry silk fibroin scaffolds for biomedical applications. *Iran Polym J (English Ed)* 22(3):143–154. <https://doi.org/10.1007/s13726-012-0113-3>
- Nagarwal RC, Kumar R, Dhanawat M, Pandit JK (2011) Modified PLA nano in situ gel: a potential ophthalmic drug delivery system. *Colloids Surf B Biointerfaces* 86(1):28–34. <https://doi.org/10.1016/j.colsurfb.2011.03.023>
- Namekawa K, Tokoro Schreiber M, Aoyagi T, Ebara M (2014) Fabrication of zeolite-polymer composite nanofibers for removal of uremic toxins from kidney failure patients. *Biomater Sci* 2(5):674–679. <https://doi.org/10.1039/c3bm60263j>
- Narasimhan L, Kuchta B, Schaefer O, Brunet P, Boulet P (2013) Mechanism of adsorption of p-cresol uremic toxin into faujasite zeolites in presence of water and sodium cations—a Monte Carlo study. *Microporous Mesoporous Mater* 173:70–77. <https://doi.org/10.1016/j.micromeso.2013.02.003>
- Naskar D, Ghosh AK, Mandal M, Das P, Nandi SK, Kundu SC (2017a) Dual growth factor loaded nonmulberry silk fibroin/carbon nanofiber composite 3D scaffolds for in vitro and in vivo bone regeneration. *Biomaterials* 136:67–85. <https://doi.org/10.1016/j.biomaterials.2017.05.014>
- Naskar D, Bhattacharjee P, Ghosh AK, Mandal M, Kundu SC (2017b) Carbon nanofiber reinforced nonmulberry silk protein fibroin nanobiocomposite for tissue engineering applications. *ACS Appl Mater Interfaces* 9(23):19356–19370. <https://doi.org/10.1021/acsami.6b04777>
- Nguyen TP et al (2019) Silk fibroin-based biomaterials for biomedical applications: a review. *Polymers* 11(12):1933. <https://doi.org/10.3390/polym11121933>
- Ninomiya H, Kawashima Y, Nagasawa T (2000) Inhibition of complement-mediated haemolysis in paroxysmal nocturnal haemoglobinuria by heparin or low-molecular weight heparin. *Br J Haematol* 109(4):875–881. <https://doi.org/10.1046/j.1365-2141.2000.02125.x>

- Page K, Wilson M, Parkin IP (2009) Antimicrobial surfaces and their potential in reducing the role of the inanimate environment in the incidence of hospital-acquired infections. *J Mater Chem* 19(23):3818–3831. <https://doi.org/10.1039/b818698g>
- Pham QP, Sharma U, Mikos AG (2006) Electrospinning of polymeric nanofibers for tissue engineering applications: a review. *Tissue Eng* 12(5):1197–1211. <https://doi.org/10.1089/ten.2006.12.1197>
- Qi P, Maitz MF, Huang N (2013) Surface modification of cardiovascular materials and implants. *Surf Coat Technol* 233:80–90. <https://doi.org/10.1016/j.surfcoat.2013.02.008>
- Qin J et al (2013) Evaluation of drug release property and blood compatibility of aspirin-loaded electrospun PLA/RSF composite nanofibers. *Iran Polym J (English Ed)* 22(10):729–737. <https://doi.org/10.1007/s13726-013-0171-1>
- Qu P, Tang H, Gao Y, Zhang LP, Wang S (2010) Polyethersulfone composite membrane blended with cellulose fibrils. *Bioresources* 5(4):2323–2336. <http://ojs.cnr.ncsu.edu/index.php/BioRes/article/view/1151>. Accessed 5 Sept 2022
- Ren Z, Chen G, Wei Z, Sang L, Qi M (2013) Hemocompatibility evaluation of polyurethane film with surface-grafted poly(ethylene glycol) and carboxymethyl-chitosan. *J Appl Polym Sci* 127(1):308–315. <https://doi.org/10.1002/app.37885>
- Sagnella S, Mai-Ngam K (2005) Chitosan based surfactant polymers designed to improve blood compatibility on biomaterials. *Colloids Surf B Biointerfaces* 42(2):147–155. <https://doi.org/10.1016/j.colsurfb.2004.07.001>
- Sahay R et al (2012) Electrospun composite nanofibers and their multifaceted applications. *J Mater Chem* 22(26):12953–12971. <https://doi.org/10.1039/c2jm30966a>
- Scopelliti PE et al (2010) The effect of surface nanometre-scale morphology on protein adsorption. *PLoS One* 5(7):e11862. <https://doi.org/10.1371/journal.pone.0011862>
- Seddiqi H et al (2021) Cellulose and its derivatives: towards biomedical applications. *Cellulose* 28(4):1893–1931. <https://doi.org/10.1007/s10570-020-03674-w>
- Seib FP, Herklotz M, Burke KA, Maitz MF, Werner C, Kaplan DL (2014) Multifunctional silk-heparin biomaterials for vascular tissue engineering applications. *Biomaterials* 35(1):83–91. <https://doi.org/10.1016/j.biomaterials.2013.09.053>
- Sell S et al (2007) Extracellular matrix regenerated: tissue engineering via electrospun biomimetic nanofibers. *Polym Int* 56(11):1349–1360. <https://doi.org/10.1002/pi.2344>
- Shao W, He J, Wang Q, Cui S, Ding B (2017) Biomineralized poly(l-lactic-co-glycolic acid)/graphene oxide/tussah silk fibroin nanofiber scaffolds with multiple orthogonal layers enhance osteoblastic differentiation of mesenchymal stem cells. *ACS Biomater Sci Eng* 3(7):1370–1380. <https://doi.org/10.1021/acsbiomaterials.6b00533>
- Sheikh FA, Barakat NA, Kim BS, Aryal S, Khil MS, Kim HY (2009) Self-assembled amphiphilic polyhedral oligosilsesquioxane (POSS) grafted poly(vinyl alcohol)(PVA) nanoparticles. *Mater Sci Eng: C* 29(3):869–876. <https://doi.org/10.1016/j.msec.2008.07.029>
- Silver JH, Lin JC, Lim F, Tegoulia VA, Chaudhury MK, Cooper SL (1999) Surface properties and hemocompatibility of alkyl-siloxane monolayers supported on silicone rubber: effect of alkyl chain length and ionic functionality. *Biomaterials* 20(17):1533–1543. [https://doi.org/10.1016/S0142-9612\(98\)00173-2](https://doi.org/10.1016/S0142-9612(98)00173-2)
- Song X, Gao Z, Ling F, Chen X (2012) Controlled release of drug via tuning electrospun polymer carrier. *J Polym Sci B Polym Phys* 50(3):221–227. <https://doi.org/10.1002/polb.23005>
- Song X, Li T, Cheng B, Xing J (2016) POSS-PU electrospinning nanofibers membrane with enhanced blood compatibility. *RSC Adv* 6(70):65756–65762. <https://doi.org/10.1039/c6ra07681e>
- Soundararajan A et al (2018) Surface topography of polylactic acid nanofibrous mats: influence on blood compatibility. *J Mater Sci Mater Med* 29(9):145. <https://doi.org/10.1007/s10856-018-6153-2>
- Sultan MT et al (2019) Recirculating peritoneal dialysis system using urease-fixed silk fibroin membrane filter with spherical carbonaceous adsorbent. *Mater Sci Eng C* 97:55–66. <https://doi.org/10.1016/j.msec.2018.12.021>



- Takeshita S et al (1994) Therapeutic angiogenesis. A single intraarterial bolus of vascular endothelial growth factor augments revascularization in a rabbit ischemic hind limb model. *J Clin Invest* 93(2):662–670. <https://doi.org/10.1172/JCI117018>
- Teng CP et al (2014) Star-shaped polyhedral oligomeric silsesquioxane-polycaprolactone-polyurethane as biomaterials for tissue engineering application. *NPG Asia Mater* 6(11):e142. <https://doi.org/10.1038/am.2014.102>
- Vogler EA (2012) Protein adsorption in three dimensions. *Biomaterials* 33(5):1201–1237. <https://doi.org/10.1016/j.biomaterials.2011.10.059>
- Voinova M, Repin N, Sokol E, Tkachuk B, Gorelik L (2019) Physical processes in polymeric filters used for dialysis. *Polymers* 11(3):389. <https://doi.org/10.3390/polym11030389>
- Wang W, Lin Guo Y, Otaigbe JU (2009) The synthesis, characterization and biocompatibility of poly(ester urethane)/polyhedral oligomeric silsesquioxane nanocomposites. *Polymer (Guildf)* 50(24):5749–5757. <https://doi.org/10.1016/j.polymer.2009.05.037>
- Weber N, Wendel HP, Ziemer G (2002) Hemocompatibility of heparin-coated surfaces and the role of selective plasma protein adsorption. *Biomaterials* 23(2):429–439. [https://doi.org/10.1016/S0142-9612\(01\)00122-3](https://doi.org/10.1016/S0142-9612(01)00122-3)
- Wei J et al (2009) Influence of surface wettability on competitive protein adsorption and initial attachment of osteoblasts. *Biomed Mater* 4(4):045002. <https://doi.org/10.1088/1748-6041/4/4/045002>
- Xu F, Li Y, Deng Y, Xiong J (2008) Porous nano-hydroxyapatite/poly(vinyl alcohol) composite hydrogel as artificial cornea fringe: characterization and evaluation in vitro. *J Biomater Sci Polym Ed* 19(4):431–439. <https://doi.org/10.1163/156856208783719473>
- Yang Y, Zhou Y, Chuo H, Wang S, Yu J (2007) Blood compatibility and mechanical properties of oxidized-chitosan films. *J Appl Polym Sci* 106(1):372–377. <https://doi.org/10.1002/app.25399>
- Yao Y et al (2014) Effect of sustained heparin release from PCL/chitosan hybrid small-diameter vascular grafts on anti-thrombogenic property and endothelialization. *Acta Biomater* 10(6):2739–2749. <https://doi.org/10.1016/j.actbio.2014.02.042>



**Rumysa Saleem Khan** was born in Srinagar, J&K, India, in 1995. She received a B.S. degree in Biochemistry in 2016 and an M.S. degree in Biotechnology from the University of Kashmir, Srinagar, in 2018 and was receiving DBT Fellowship. From 2019 to 2020, she was a JRF with a biochemical engineering lab at NIT, Srinagar, where she received MHRD Junior Research Fellowship.

She is currently pursuing a Ph.D. degree under the supervision of Dr. Faheem A. Sheikh at the University of Kashmir, Srinagar, J&K, India, and is receiving the Science and Engineering Research Board (SERB) Fellowship. She is currently the author of 16 scientific articles published in international journals. Ms. Khan's research interests include the biomimicking of biological molecules in the lab, the fabrication of biocompatible scaffolds for tissue engineering, nanofiber formation for wound healing and bone regeneration, and exploiting the roles of different nanoparticles in tissue engineering. She also has expertise in mammalian cell culture and molecular biology techniques.



**Anjum Hamid Rather** was born in J&K, India, and studied for her M.Sc. in the Department of Bioresources, University of Kashmir, Srinagar, JK. She qualified for the CSIR-UGC NET in 2019 and was awarded a National Fellowship by the University Grants Commission (UGC) in 2020 to pursue her Ph.D. research for 5 years.

She is currently pursuing her Ph.D. degree in the Department of Nanotechnology, University of Kashmir, Srinagar, J&K, under the supervision of Dr. Faheem A. Sheikh. Her interests include developing polymeric nanofibers for advanced tissue engineering, wound healing applications, and exploiting the role of different nanoparticles and essential oils in tissue engineering. She has contributed to 13 peer-reviewed articles and 4 book chapters.



**Taha Umair Wani** received his bachelor's degree in Pharmacy from the University of Kashmir, India, in 2012 and his master's in Pharmaceutics from Punjab Technical University, Punjab, India, in 2014. He completed his Ph.D. in Pharmaceutics from the University of Kashmir, India, in 2020.

He is currently working as a research associate in the Department of Nanotechnology, University of Kashmir. He is the author of more than 40 publications. His research interests include drug formulation development, preclinical research, nanomedicine, and biomaterial fabrication. He has expertise in cell culture studies, antimicrobial assays, drug delivery, in vivo experiments, and pharmacokinetic studies.



**Muheeb Rafiq** was born and raised in Srinagar, J&K, India. He received his B.Sc. degree from the University of Kashmir in 2017. Later in 2012, he completed his M.Sc. in Nanotechnology from the University of Kashmir. During his master's, he gained a hands-on experience in the research area as he worked as an intern for 6 months under Dr. Mushtaq (Asst. Prof., Dept of Nanotechnology, University of Kashmir). After completing his master's, he started working on a project funded by the Council of Scientific and Industrial Research (CSIR) under the supervision of Dr. Faheem A. Sheikh (Asst. Prof., Dept of Nanotechnology, University of Kashmir).

He is currently enrolled in a Ph.D. program and is working under the mentorship of Dr. Faheem A. Sheikh. He has authored a 5 publications, including research papers and review articles. His research interests include the fabrication of biocompatible nanofibers and nanoporous scaffolds for hard and soft tissue engineering, the biological synthesis of nanoparticles, and post-modification of nanofibers.

**Touseef Amna** received her Ph.D. in Microbiology in 2006 from Aligarh Muslim University (AMU, Central University), India. Presently, she is working as an associate professor at Albaha University, Saudi Arabia. During her research career, she got the opportunity to spend postdoctoral stages at the University of Dortmund, Germany; Universidad de Talca, Chile; and Chonbuk National University, South Korea, and received various prestigious awards and grants. She authored two patents (one US patent and one Korean) and more than 100 research articles in journals of

international repute. She is an editor, guest editor, and editorial board member of various national and international journals. Her research interests consist of the design and synthesis of biocompatible scaffolds for antimicrobial applications, cell culture, and tissue engineering.



**M. Shamshi Hassan** is working as an associate professor in the Faculty of Science Albaha University, Saudi Arabia. He was awarded an international fellowship to pursue his doctoral degree and received his Ph.D. in Chemical Engineering from the Department of Chemical Engineering, Chonbuk National University, South Korea, in 2010. After his Ph.D. he has been awarded Postdoctoral Fellowship (PDF) by the Textile and Fiber Engineering Department of CBNU, South Korea. His research interests include the synthesis of pure and hybrid metal oxides (quantum dots or nanocrystals, 1D, 2D, 3D, and flower-shaped morphology), nanostructured materials, or nanofibers and their application in supercapacitors and as biological/chemical disinfectants.



**Syed Mudasir Ahmad** is a professor and head of the Division of Animal Biotechnology, Faculty of Veterinary Sciences and Animal Husbandry, Shuhama, SKUAST-Kashmir. He has a teaching experience of 15 years. His research experience spans more than two decades, and he has published around 100 research articles in reputed journals.



**Shafquat Majeed** is currently working as an assistant professor in the Department of Nanotechnology, University of Kashmir, India. Dr. Majeed did his master's in Chemistry from the Department of Chemistry, University of Kashmir. He did his Ph.D. at the prestigious Indian Institute of Science Bangalore (2008–2015). He has a postdoctoral research experience in rare-earth-based nanomaterials for biomedical applications and the fabrication of perovskite-based solar cells from the Centre for Nanoscience and Engineering, IISc Bangalore (2015–2016). He heads the laboratory, where they work on the synthesis, characterization, and optical and magnetic properties of nanomaterials prepared through various solution-based routes. More specifically, they are working on developing new and enhanced multimodal imaging modalities for biomedical and healthcare applications.



**Mushtaq A. Beigh** is working as an assistant professor at the Department of Nanotechnology, University of Kashmir, India. Dr. Beigh has postdoctoral research experience in cellular signaling and disease modeling (2013–2016). He completed his Ph.D. at the University of Kashmir, India (2008–2012). He heads a laboratory at the University of Kashmir, where they work on a bio-nano interface to understand the molecular basis of nanoconjugate internalization. They also try to understand the growth factor signaling inputs directed at multiple cellular receptors, like NRP1 and integrins, in order to work out the mechanistic details of receptor-based internalization.



**Faheem A. Sheikh** is an assistant professor at the Department of Nanotechnology, University of Kashmir, India (2015). He served as an assistant professor at the Department of Biotechnology at the Central University of Kashmir, India (2015–2016); a research professor at Myongji University, South Korea (2014–2015); an assistant professor at Hallym University, South Korea (2012–2014); a postdoc/research fellow at the University of Texas Rio Grande Valley, Texas, United States of America (2010–2012); and a research professor at Myongji University, South Korea (2010). His research mainly focuses on fabricating nanomaterials used in tissue engineering.